Journal of Neurocytology **32**, 229–243 (2003)

Effects of congenital deafness in the cochlear nuclei of *Shaker-2* mice: An ultrastructural analysis of synapse morphology in the endbulbs of Held

DANIEL J. LEE[1], HUGH B. CAHILL[2] and DAVID K. RYUGO[1,2*]

Center for Hearing Sciences, Departments of Otolaryngology-Head and Neck Surgery[1] and Neuroscience[2], Johns Hopkins University School of Medicine, Baltimore, MD 21205, USA
dryugo@bme.jhu.edu

Received 7 March 2003; revised 26 June 2003; accepted 26 June 2003

Abstract

It is well established that manipulation of the sensory environment can significantly alter central auditory system development. For example, congenitally deaf white cats exhibit synaptic alterations in the cochlear nucleus distinct from age-matched, normal hearing controls. The large, axosomatic endings of auditory nerve fibers, called endbulbs of Held, display reduced size and branching, loss of synaptic vesicles, and a hypertrophy of the associated postsynaptic densities on the target spherical bushy cells. Such alterations, however, could arise from the cat's genetic syndrome rather than from deafness. In order to examine further the role of hearing on synapse development, we have studied endbulbs of Held in the *shaker-2* (*sh2*) mouse. These mice carry a point mutation on chromosome 11, affecting myosin 15 and producing abnormally short stereocilia in hair cells of the inner ear. The homozygous mutant mice are born deaf and develop perpetual circling behavior, although receptor cells and primary neurons remain intact at least for the initial 100 days of postnatal life. Endbulbs of Held in 7-month old, deaf *sh2* mice exhibited fewer synaptic vesicles in the presynaptic ending, the loss of intercellular cisternae, and a hypertrophy of associated postsynaptic densities. On average, postsynaptic density area for *sh2* endbulbs was $0.23 \pm 0.19\ \mu m^2$ compared to $0.07 \pm 0.04\ \mu m^2$ ($p < 0.001$) for age-matched, hearing littermates. These changes at the endbulb synapse in *sh2* mice resemble those of the congenitally deaf white cat and are consistent with the idea that they represent a generalized response to deafness.

Introduction

The impact of environmental cues on normal brain development has been demonstrated in several systems, including the visual (Wiesel & Hubel, 1963; LeVay *et al*., 1980; Goodman & Shatz, 1993), somatosensory (Van der Loos & Woolsey, 1973; Killackey *et al*., 1976; Juliano *et al*., 1994), and olfactory (Meisami, 1978; Benson *et al*., 1984; Elkabes *et al*., 1993). These observations are consistent with the notion of "environmental nurturing" of brain development, where sensory deprivation abnormally alters neural growth, maturation, and function (Neville & Bavelier, 2002; Binns *et al*., 2002; Tibussek *et al*., 2002). In the central auditory system, for example, acoustic deprivation results in cell shrinkage, dendritic atrophy, abnormal response properties, and synaptic changes (Powell & Erulkar, 1962; Benes *et al*., 1977; Trune, 1982a,b; Deitch & Rubel, 1984, 1989a,b; Gold & Knudsen, 1999; Leake *et al*., 1997; Moore *et al*., 1989). These studies, however, examined phenotypically normal hearing subjects undergoing cochlear ablation or pharmacologic poisoning. Consequently, interpretations are complicated by the potential for nonspecific changes caused by surgical trauma or ototoxic drug effects. Alternatively, there are mammalian models of congenital deafness that provide an opportunity to examine the effects of a natural form of sound deprivation on the development of the central auditory system.

Congenital deafness has been shown to affect neuronal maturation in the deaf white cat. The deaf white cat is characterized by early-onset cochleosaccular degeneration, heterochromic irides, and relatively long white fur (Bergsma & Brown, 1971; Mair, 1973). There is concomitant severe, sensorineural hearing loss associated with neuronal changes in the spiral ganglion and central auditory pathway (Bosher & Hallpike, 1965; Suga & Hattler, 1970; Mair, 1973; West & Harrison, 1973;

*To whom correspondence should be addressed.

0300–4864

Pujol *et al*., 1977; Rebillard *et al*., 1981a,b; Schwartz & Higa, 1982; Larsen & Kirchoff, 1992; Saada *et al*., 1996). In the cochlear nucleus, there are also conspicuous reductions in the size of auditory nerve endings, loss of synaptic vesicles, and hypertrophy of certain postsynaptic densities (Ryugo *et al*., 1997, 1998; Redd *et al*., 2000). Thus the congenitally deaf white cat presented a naturally occurring model for the study of the effects of auditory deprivation on the brain.

These alterations in neuronal morphology, however, may represent characteristics of the genetic syndrome for the deaf white cat rather than changes resulting from deafness. Indeed, the specific genetic alterations underlying the deaf white cat phenotype are unknown. We therefore examined the *shaker-2* (*sh2*) mouse as an alternative model for congenital deafness. The *sh2* mouse has a recessive point mutation within exon 18 of the *Myo15* gene, located on murine chromosome 11 (Probst *et al*., 1998, 1999; Liang *et al*., 1999). This guanine-to-adenosine transition results in a cysteine to tyrosine substitution within a highly conserved motor domain, producing a disruption of the organization of actin in the stereocilia of receptor cells of the organ of Corti and vestibular end organ (Probst *et al*., 1998; Anderson *et al*., 2000; Beyer *et al*., 2000). Homozygous mutants (*sh2/sh2*) possess stubby stereocilia, are phenotypically deaf, and exhibit circling behavior. The hair cells and primary ganglion cells remain for approximately the first 100 postnatal days before they begin to atrophy and disappear (Deol, 1954; Webster *et al*., 1986; Probst *et al*., 1998). Thus the *sh2* mouse conceivably represents a less complicated form of congenital deafness and has been used to study the effects of early postnatal cochlear degeneration on the maturation of auditory nuclei of the brain stem (Webster *et al*., 1986). In this context, we investigated auditory nerve synapses with the hypothesis that if the congenitally deaf mouse exhibits synaptic changes resembling those of congenitally deaf cats, then we could infer with confidence that deafness produced these changes in both species.

In the present study, we genotyped our subjects, tested their hearing using ABR techniques, and studied the synaptic morphology of endbulbs of Held. We observed a loss of synaptic vesicles in the presynaptic endings and a hypertrophy of the associated postsynaptic densities in deaf *sh2/sh2* mice, compared with normal hearing wild type (+/+) and heterozygous (+/*sh2*) mice. These results are virtually identical when comparing congenital deaf white cats to normal hearing cats. Since the cat and mouse models have different genetic backgrounds and mutations, the data suggest that sensory hearing loss *per se* produce these synaptic abnormalities in the auditory nerve endings and spherical bushy cells.

Materials and methods

SUBJECTS

One-month old heterozygous (+/*sh2*) normal hearing and homozygous *(sh2/sh2)* deaf mice were obtained from a licensed vendor (Jackson Laboratories, Bar Harbor, ME). These mice were used as breeders to establish a colony of normal hearing and deaf *sh2* mice. The data in this report are from mice derived from the colony and include five normal hearing and three deaf *sh2* mice, all 7 months of age. Subjects exhibited normal respiratory function, intact tympanic membranes, and had no signs of outer or middle ear infections (Table 1). All procedures were approved and performed in accordance with the guidelines of the Animal Care and Use Committee of the Johns Hopkins School of Medicine.

PHYSIOLOGIC TESTING

The hearing of test subjects was initially assessed with the startle reflex, generated by a hand clap or finger snap behind the mouse. Heterozygous (+/*sh2*) mice exhibited a distinct startle response, whereas homozygous (*sh2/sh2*) mice were unresponsive. Standard ABR testing was then performed. Subjects were anesthetized with intraperitoneal injections of a solution containing a mixture of ketamine (25 mg/kg) and xylazine (2.5 mg/kg). A small amount (0.1 ml) of 1% Lidocaine was infiltrated in the postauricular region and scalp. ABRs were recorded in response to clicks, utilizing a vertex electrode and an electrode placed behind the pinna ipsilateral to the tested ear. Click levels were determined in dB peak equivalent SPL (dB peSPL) using a calibrated microphone and

Table 1. *Shaker-2* Mouse subject data.

Subject	*Age*	*Sex*	*Weight (gms)*	*Startle reflex*	*ABR threshold (dB peSPL)*	*Behavioral status*	*Genotype*
1	7 months	Female	23.7	Present	31.2	Non-spinner	+/*sh2*
2	7 months	Female	28.0	Present	29.9	Non-spinner	+/*sh2*
3	7 months	Female	27.0	Present	43.8	Non-spinner	+/*sh2*
4	7 months	Female	33.5	Present	28.5	Non-spinner	+/*sh2*
5	7 months	Female	31.0	Present	29.4	Non-spinner	+/+
6	7 months	Female	29.5	Absent	NR	Spinner	*sh2/sh2*
7	7 months	Female	22.5	Absent	NR	Spinner	*sh2/sh2*
8	7 months	Male	27.0	Absent	NR	Spinner	*sh2/sh2*

NR, no response to 100 dB clicks.

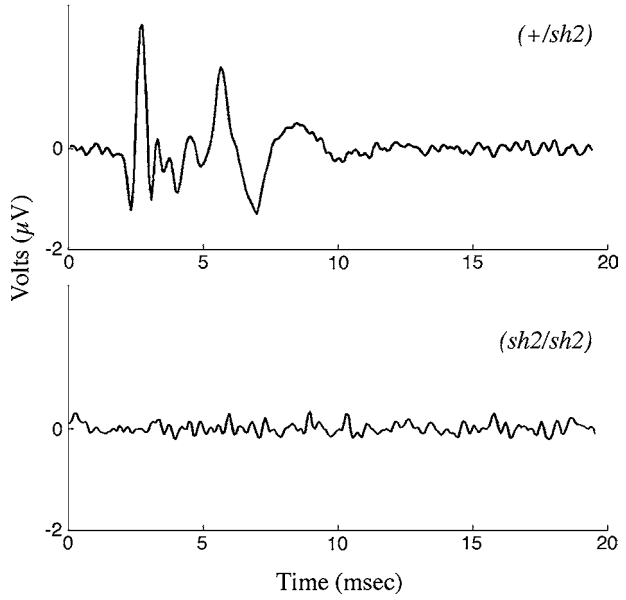

Fig. 1. Representative auditory brainstem evoked responses (ABRs) from a normal hearing, 7 month old +/*sh2* mouse (top) and a 7 month old *sh2/sh2* littermate (bottom) in response to 80 dB clicks. Heterozygous (+/*sh2*) and wildtype (+/+) mice exhibited normal ABR thresholds and waveforms to click stimuli, with a mean threshold of 32.6 ± 6.4 dB peSPL. In contrast, clicks up to 100 dB peSPL failed to elicit ABR waveforms in the three homozygous (*sh2/sh2*) mice.

referenced to a 1 kHz continuous tone (Burkard, 1984). Clicks of 100 μs duration ($n = 500$) and alternating polarity were presented in 5 dB increments, starting at 0 dB and progressing to 100 dB peSPL. ABRs were recorded over 20 ms and then averaged for each intensity level (Tucker Davis Technologies, Gainesville, FL). Representative ABR waveforms are shown (Fig. 1). Threshold values were determined by comparing the largest positive waveform between 2.5 to 7.5 msec after the stimulus to the background response. The background amplitudes were measured 15–20 msec after the stimulus and averaged. The sound pressure level for which an evoked response exceeded background levels by two standard deviations was defined as the hearing threshold. A summary of ABR data is shown in Table 1.

AUDITORY NERVE INJECTIONS

Immediately following ABR testing, each mouse was anesthetized with an intraperitoneal injection of ketamine (25 mg/kg) and xylazine hydrochloride (2.5 mg/kg). When the mouse was areflexic to paw pinch, it was secured in a head holder with the left ear facing up. A left postauricular incision was made, and the soft tissue posterior to the external auditory canal was dissected free from the canal. An incision was made into the canal near the bulla, allowing visualization of the tympanic membrane. The tympanic membrane, malleus and incus were removed, and the postero-inferior aspect of the bulla was chipped away using a fine-tipped rongeur and diamond bit drill with a 0.5 mm tip diameter. The stapedial artery, which usually traverses the stapes footplate, was cauterized at its superior and inferior limits using a bipolar electric cautery. The stapes was removed from the oval window. A right angle hook was placed into either the round or oval window, and the lateral wall of the otic capsule was removed by gentle picking with the hook. The modiolus of the cochlea was located, and a hole made into its core between the basal turn and apical half-turn using a size 0.01 (100 μm) insect pin. A glass electrode with an inner diameter of 5–20 μm filled with a 5% neurobiotin solution in 0.1 M potassium chloride was placed into the hole made by the insect pin. Neurobiotin was injected into the modiolus by passing 5 μA of positive current (50% duty cycle) for 0.5–10 minutes through the micropipette. Following the injection, the electrode was removed, incisions were closed, and the animal was allowed to recover for up to six hours.

TISSUE PREPARATION

At the end of the survival period, a lethal dose of sodium pentobarbital was administered and the animal was perfused through the heart with 5 ml of 0.1 M cacodylate-buffered saline (pH 7.3) containing 1% sodium nitrite, followed by approximately 200 ml of 0.1 M cacodylate-buffered fixative (pH 7.2) containing 2% glutaraldehyde and 2% paraformaldehyde. The fixative solution was perfused for approximately 10 minutes, and the skin and cranium were removed using an operating microscope to expose the brainstem, cerebellum and cochleae. Each cochlea was gently perfused by flushing the same fixative into the round window and draining it from the oval window. A fine wire needle (0.25 mm in diameter) was inserted into the right side of the brain stem, parallel to the long axis, for orientation purposes. The partially dissected head was postfixed overnight at 4°C in the same fixative solution.

The following day, the brain stem was dissected from the skull, separated from the cerebellum and forebrain, blocked with a razor blade to include both cochlear nuclei, and embedded in gelatin-albumin hardened with glutaraldehyde. The gelatin-albumin block was trimmed, mounted, and sectioned with a Vibratome in the coronal plane at a thickness of 75 μm. The cochleae were trimmed of excess soft tissue and decalcified by daily changes with a solution of 0.1 M EDTA and 0.5% glutaraldehyde. When decalcified, each cochlea was dehydrated, infiltrated with Araldite, and sectioned on a rotary microtome at a thickness of 20 μm. Sections were stained with Toluidine Blue and coverslipped with Permount.

All brain sections were collected in 0.1 M cacodylate buffer (CB, pH 7.3) and then incubated in a solution of ABC Elite (Vector Laboratories) in 0.1 M CB overnight at 4°C. The next morning, sections were rinsed several times in 0.1 M CB, incubated in the dark for 60 minutes in a 0.05% solution of cacodylate-buffered 3,3′-diaminobenzidine (DAB, grade II, Sigma, St. Louis, MO) activated with 0.01% hydrogen peroxide, and rinsed several more times with 0.1 M CB.

These sections were processed for electron microscopy by placing the tissue in 1% OsO_4 for 15 minutes, rinsing several times in 0.1 M maleate buffer (pH 5.0) and staining in 1% uranyl acetate (4°C) overnight. The following morning, the sections were washed with 0.1 M maleate buffer, dehydrated in increasing concentrations of ethanol, soaked in propylene oxide, infiltrated with EPON, and embedded in fresh EPON between sheets of Aclar (Ted Pella, Inc., Redding, CA). Hardened sections were taped to labeled glass slides for

light microscopic review. Selected areas in the anteroventral cochlear nucleus (AVCN) were traced with a drawing tube and/or photographed with the aid of a light microscope, with particular attention paid to labeled endbulbs.

Relevant segments of AVCN were identified, dissected from Aclar-embedded brain stem sections and reembedded in BEEM capsules for sectioning and electron microscopic analysis. Serial sections of approximately 75 nm thickness were collected on Formvar-coated grids, stained with 7% uranyl acetate, and viewed and photographed with a JEOL 100CX electron microscope. Magnifications ranged from $\times$2,700 to $\times$14,000. Because each ultrathin section represents a thin slice across neuronal structures, only a representative portion appears in any given section. Portions of endbulbs are referred to as profiles, and multiple series of consecutive sections (10–25) were reconstructed and analyzed.

The negatives of electron micrographs were scanned and digitized (Leafscan 45, Leaf Systems, Inc.), the contrast and/or exposure adjusted as needed (Adobe Photoshop 5.0), and images printed in high-resolution format on archival photographic paper (Epson Stylus Photo 1280).

SEQUENCING ANALYSIS

All subjects in this study were genotyped to assess for mutations of *Myo15* on murine chromosome 11. Approximately 0.5 cm of tail was harvested prior to transcardial perfusion and stored at -20°C. DNA purification from this tissue was performed following the manufacturer's protocol using a standard extraction kit (DNeasy^{TM} Tissue Kit, Qiagen, Inc.). Purified DNA preparations yielded concentrations of approximately 200 ng/μl. Flanking, single-stranded oligonucleotide primers were designed based on previously published sequencing data of exon 18 of *Myo15* (Probst *et al*., 1998). The forward primer was 5′-GTAGCACACCTTTTCTCCAG-3′ and the reverse primer was 5′-AGTGCCACACTTCA-3′. Five nanograms of template were used in a master mix with Taq polymerase (Invitrogen Life Technologies, Carlsbad, CA) to a volume of 50 μl. A standard PCR thermocycler (GeneAmp PCR system 2400, Perkins Elmer) was used for 30 cycles of DNA amplification (95°C for 2 minutes, 59°C for 30–60 seconds, and 74°C for 1–2 minutes). Fifty μl of each PCR product was subjected to electrophoresis on a 2% agarose gel with a 100 base pair (bp) ladder. The gels reveal 355 bp bands that correspond to the amplified sequence of exon 18 of *Myo15*. These bands were individually excised followed by gel-purification of these PCR products (QIAquick^{TM} Gel Extraction Kit, Qiagen, Inc.). Utilizing these purified PCR products and a 5′ oligonucleotide primer (5′-GACCTGGTGGAAAAGATGG-3′), automated sequencing of exon 18 was performed on the region flanking codon 674 by the DNA Analysis Facility at the Johns Hopkins University (Fig. 2).

DATA ANALYSIS: ELECTRON MICROSCOPY

Electron microscopic analysis was directed on the most anterior region of the AVCN. In the adult mouse, this region is heavily populated with endbulbs of Held and spherical bushy cells (Webster & Trune, 1982; Willard & Ryugo, 1983; Limb & Ryugo, 2000). Spherical bushy cells are recognizable by round-to-oval cell bodies, centrally-placed, pale nucleus, perinuclear cap of rough endoplasmic reticulum, and association with endbulbs. Endbulbs are characterized by their pale cytoplasm, content of clear, round synaptic vesicles, and association with convex, asymmetric postsynaptic densities (PSDs). Characterization of labeled endbulbs allowed us to analyze unlabeled endbulbs with confidence.

Consecutive, unbroken series of ultrathin sections were collected and photographed. Morphometric analysis (Image Processing Toolkit, Reindeer Games, Inc., Asheville, NC) included profile area, mitochondrial fraction (ratio of mitochondrial area to cytoplasmic area), mitochondrial density (number per μm^2), vesicular density (number per μm^2), and active zone size from reconstructed and rotated PSDs.

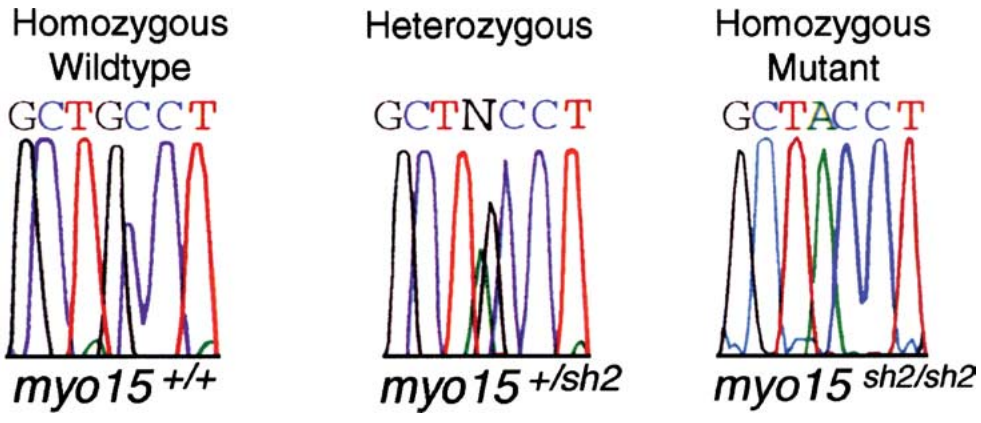

Fig. 2. DNA sequencing analysis through codon 674 of *Myo15*, exon 18. A portion of the sequencing histogram is shown. Wildtype mice (left) retained both normal alleles (+/+), whereas heterozygous *sh2* mice (middle) demonstrated a guanine (G, in black) to adenosine (A, in green) transition in 50% of alleles, consistent with a *+/sh2* genotype. Guanine and adenosine indicate that both a normal and mutant allele is present. Deaf *sh2* mice possessed homozygous mutations of *Myo15* (right). When present in both alleles, this point mutation (guanine $\rightarrow$ adenosine) results in a cysteine to tyrosine substitution within a highly conserved motor domain of the unconventional myosin 15 protein, disrupting the organization of actin in the organ of Corti and vestibular hair cells (Probst *et al*., 1998). Sequencing was performed on all test subjects to confirm genotype status.

Ending profiles and PSDs were serially reconstructed from electron micrographs. The PSD was identified as an asymmetric thickening of the postsynaptic membrane associated with the accumulation of presynaptic vesicles (Cant & Morest, 1979; Fekete *et al*., 1984). Consecutive ending profiles and active zones were traced and aligned (NIH Image Version 1.61), and the resulting "stack" was rendered into a three-dimensional structure, rotated and viewed *en face* (VoxBlast, VayTek, Inc., Iowa City, IA). Because PSDs sometimes extended beyond the series of reconstructed sections, their absolute size could not always be determined. Statistical data comparison between normal hearing controls (+/*sh2* and +/+) and deaf *sh2* mice *(sh2/sh2)* were conducted by factorial ANOVA (Statview 5.0.1, SAS Institute Inc., Cary, NC). *P* values are provided when appropriate.

Results

This report is based on 7-month old mice ($n = 8$). Test subjects exhibiting a normal acoustic startle reflex and no circling behavior ($n = 5$) were found to be heterozygous *(+/sh2)* or wildtype *(+/+)*, whereas behaviorally deaf and circling mice ($n = 3$) were homozygous *(sh2/sh2)* for the *sh2* genotype. Wildtype and heterozygous *sh2* mice had normal ABR thresholds (32.6 ± 6.4 dB peSPL) but the homozygous mice were completely unresponsive (Table 1).

Analysis of Rosenthal's canal revealed that the hearing mice (+/+ and +/*sh2*) displayed "normal looking" inner ears with mostly a full complement of spiral ganglion cells (Fig. 3, top). There was probably some cell loss due to the normal aging process, as the mice were 7 months old. By contrast, the deaf mice *(sh2/sh2)* were missing up to 50% of their ganglion cells (Fig. 3, bottom). The loss was not uniform along the length of the canal, nor was it symmetrical between left and right ears. Typically, however, the base of the canal was affected most severely and the middle and apical turns only moderately.

Neurobiotin-labeled type I auditory nerve fibers could be seen as they emanated from the injection site in the auditory nerve. Individual fibers were followed using a light microscope from the bifurcation point, along the ascending branch, and to their termination site in the anterior AVCN. Each fiber terminated by forming an endbulb of Held. Endbulbs are large, highly arborized synaptic endings that encircle up to half the somata of spherical bushy cells (Lorente de Nó, 1981; Ryugo & Fekete, 1982).

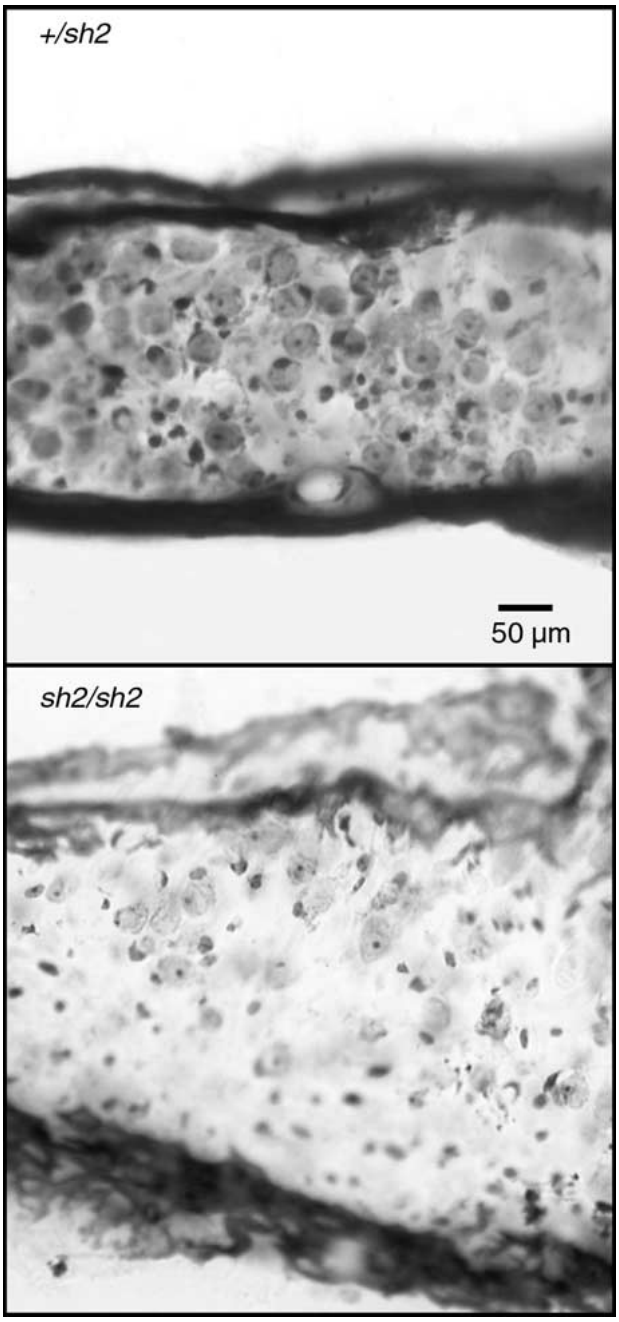

Fig. 3. Photomicrographs of Rosenthal's canal, illustrating the representative ganglion cell population in the lower apical turn of 7 month-old mice. The hearing (+/*sh2*) mouse exhibited a nearly full complement of ganglion cells. In contrast, the deaf (*sh2/sh2*) mouse revealed considerable cell loss. Ganglion cell density was normal in the apex of the canal, whereas the base exhibited severe cell loss. This pattern of graded cell loss proceeding from the base and extending about halfway to the apex was typical. The presence of the ganglion cells is sufficient to account for the primary endings in the cochlear nucleus.

ULTRASTRUCTURAL FEATURES

Spherical bushy cells were identified using previously defined criteria (Limb & Ryugo, 2000), the most obvious of which is their association with endbulbs (Fig. 4). In addition, they have a round-to-oval cell body, a large, centrally located nucleus with a smooth contour, and a nuclear cap of endoplasmic reticulum arranged in stacks, extending into the perikaryon. Endbulb synapses from normal hearing mice contain large round vesicles and numerous mitochondria (Fig. 5). The asymmetric PSDs are prominent, dome-shaped,

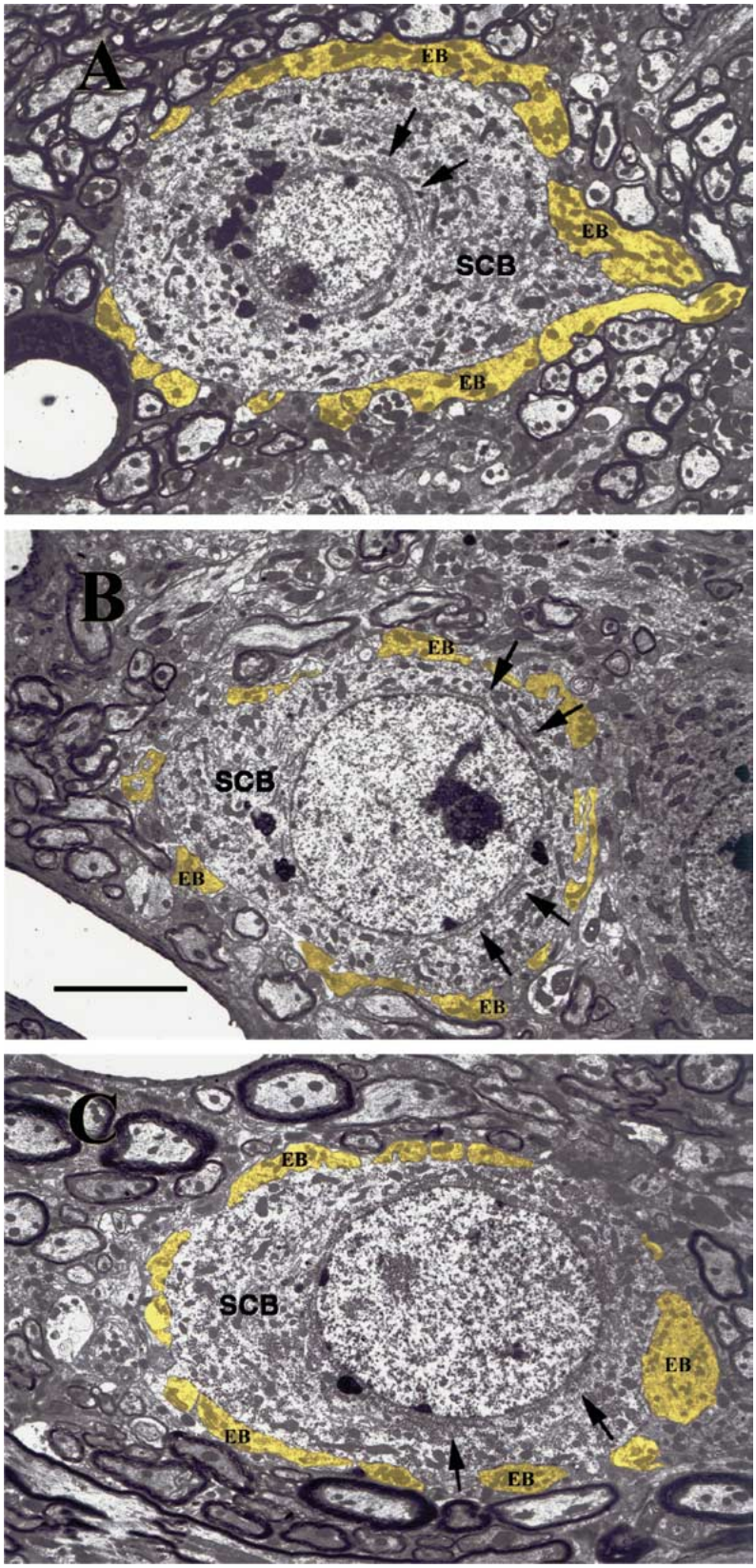

Fig. 4. Representative, low magnification electron micrographs of spherical bushy cells from 7 month old +/+ (A), +/*sh2* mice (B), and deaf, *sh2*/*sh2* mice (C). The spherical bushy cells (SBC) are concentrated in the anteroventral cochlear nucleus and receive most of their auditory input from type I auditory nerve fibers. Individual auditory nerve fibers terminate on the SBC as endbulbs of Held (EB, yellow) where each endbulb forms multiple synapses. The characteristic "Nissl" cap is represented by stacks of perinuclear rough endoplasmic reticulum (arrows). Scale bar equals 5.0 μm.

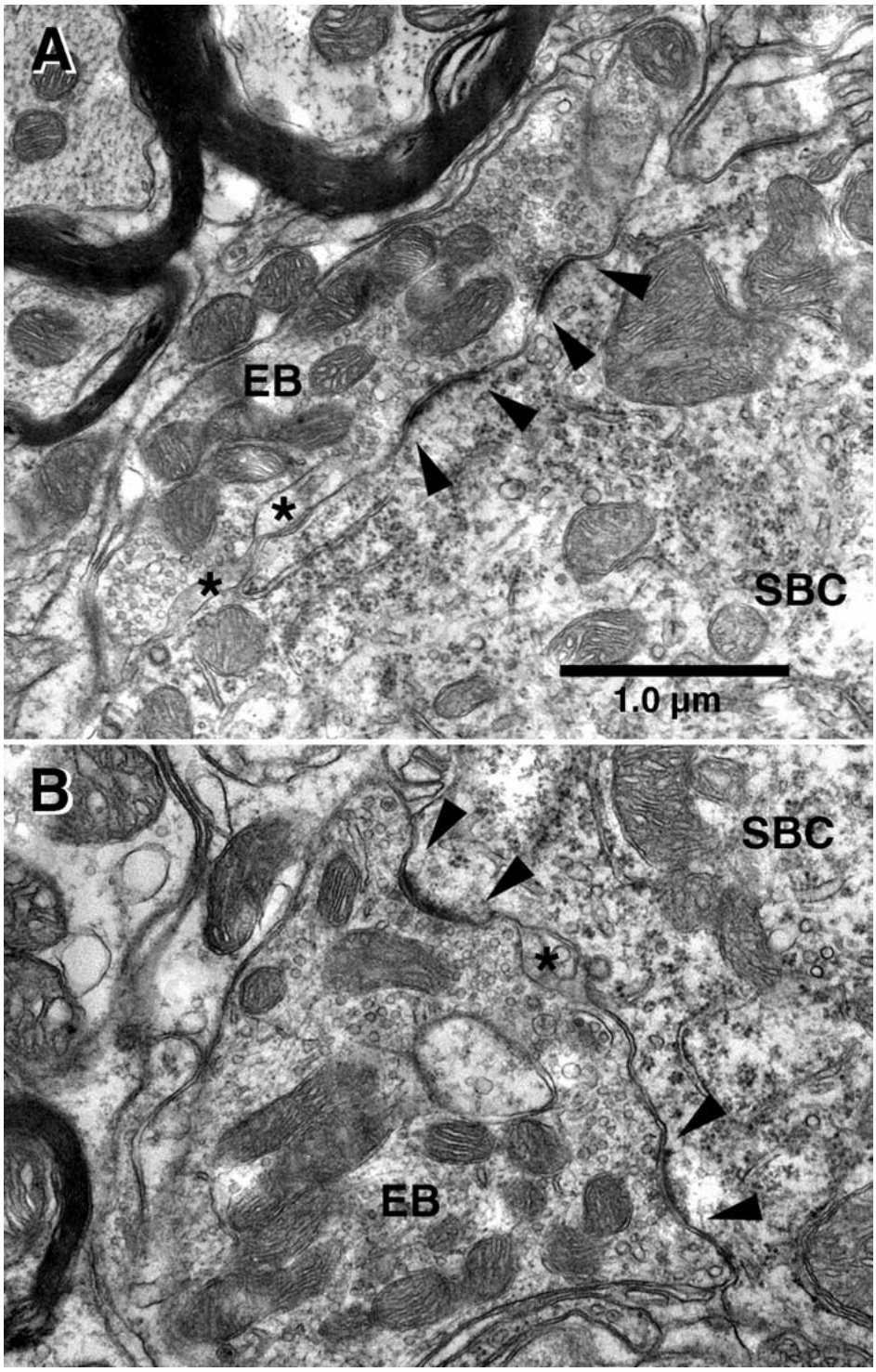

Fig. 5. Representative electron micrographs from 7 month old normal hearing, heterozygous *(+/sh2)* and wildtype (+/+) s*h*2 mice. (A) This micrograph illustrates a *+/sh2* endbulb profile (EB) that is filled with mitochondria and large round vesicles and which contacts a spherical bushy cell (SBC). Several asymmetric membrane thickenings, called postsynaptic densities (PSDs), are present. The PSD is associated with a punctate, dome-shaped convexity that protrudes into the endbulb. Synaptic vesicles lie in close association with the membrane specializations, indicating the presence of synapses (arrowheads). A separation of the pre- and postsynaptic membranes creates an intercellular channel or cistern (asterisks). These spaces may represent a site where neurotransmitter diffuses away from the synapse or where transmitter is taken up and inactivated and/or recycled. (B) Micrograph from a wild type *sh2* mouse (+/+) illustrates typical, dome-shaped synapses (arrowheads) and an intercellular cistern (asterisk). Note the characteristic curved PSDs, numerous large round vesicles, and abundant mitochondria. There is no detectable difference in endbulb morphology between the +/+ mouse and the *+/sh2* littermates. Scale bar = 1.0 μm.

and bulge into the endbulb. The PSD is a specialized cytoskeletal structure reiterating the shape of the active zone and extending into the cytosol (Sheng, 2001). This punctate membraneous convexity is characteristic for endbulb synapses in mammals (Lenn & Reese, 1966; Ryugo & Parks, 2003).

Clear differences were observed in the endbulbs of deaf *sh2/sh2* mice compared with normal hearing littermates. First, the PSDs were conspicuously larger with diminished curvature (Fig. 6). Serial section EM analysis provided direct confirmation of these changes observed in random sections. Endbulb profiles were selected from both *sh2/sh2* and +/*sh2* mice, and an unbroken series of 15–25 ultrathin EM sections were digitized, traced, and aligned. The resulting image "stack" for a given ending was rotated and viewed *en face*. This procedure yielded a view of the PSDs as they lay upon the surface of the cell body beneath the endbulb segment. *En face* views of PSDs were generated from wild type (+/+), heterozygous (+/*sh2*), and homozygous (*sh2/sh2*) mice (Fig. 7). In the deaf *sh2/sh2* mice, PSDs were hypertrophied. There was no difference in PSD size between the hearing wild type and heterozygous mice, but the average PSD area for deaf mice was larger ($0.23 \pm 0.19\ \mu m^2$) than that of age-matched, hearing littermates ($0.07 \pm 0.04\ \mu m^2$; $p < 0.001$).

Second, the average number of synaptic vesicles in endbulbs was significantly smaller in deaf compared to that of hearing mice. Many but not all primary endings exhibited a reduction in synaptic vesicles. Mean vesicular density for deaf *sh2* mice was 21 ± 9 per μm^2, compared with 77 ± 26 per μm^2 for normal hearing +/*sh2* and +/+ mice (Table 2, $p < 0.001$).

Alterations of metabolic activity with prolonged deafness may give rise to abnormalities in mitochondria number or cristae architecture. Ultrastructurally, there were no apparent differences in mitochondrial membrane or cristae morphology, but individual mitochondria were smaller, on average, when comparing endbulbs of hearing versus deaf mice. Mitochondria of deaf mice were $0.84 \pm 0.6\ \mu m^2$, whereas those of hearing mice were $0.134 \pm 0.09\ \mu m^2$ ($p < 0.001$). Mean mitochondrial volume fraction (mitochondrial area divided by cytoplasmic area) was also smaller in deaf mice (0.14 ± 0.05) when compared to hearing mice (0.25 ± 0.07, $p < 0.001$). These observations are consistent with decreased metabolic activity at the synapses of deaf animals (Lippe *et al*., 1980).

The synaptic interface in normal hearing mice is marked by the presence of small separations formed between the pre- and postsynaptic membranes (Figs. 5 and 8). When reconstructed in three dimensions, these areas of "non-apposition" between membranes were observed to form intermembraneous cisternae or tunnels of extracellular space. Occasionally, a thin, finger-like glial process extends into the cistern. These cisternae between endbulb and spherical bushy cell, however, were virtually absent among the deaf *sh2/sh2* mice (Fig. 6).

The relationship between the endbulb and spherical bushy cell was defined by another membrane specialization. Regions of electron-dense plaques with symmetric projections on both the pre- and postsynaptic membrane were often observed near synaptic junctions. These puncta adherentia were not reliably associated with the clustering of synaptic vesicles and are inferred to assist in the maintenance of the structural integrity of synaptic connections (Fig. 8). Puncta adherentia were numerous in both deaf and hearing *sh2* mice.

Although the sample size is small, there were variable differences when comparing features between the wildtype mouse and its heterozygous littermates. Both mice could hear with equal sensitivity. PSD area was $0.06 \pm 0.03\ \mu m^2$ for the wildtype mouse and $0.07 \pm 0.04\ \mu m^2$ for +/*sh2* mice with normal hearing ($p = 0.58$). In contrast, the mean vesicular density for wild type mice was 63 ± 12 per μm^2 compared with 77 ± 26 per μm^2 for the heterozygous littermates ($p = 0.07$). Finally, there was no statistically significant difference in mitochondrial fraction or mitochondrial density between the wildtype mouse and its heterozygous littermates (Table 2).

Discussion

Normal hearing, 7-month old *shaker-2* (+/+) mice exhibit synaptic architecture in their endbulbs of Held that is consistent with observations reported for adult cats (Ibata & Pappas, 1976; Cant & Morest, 1979; Ryugo & Fekete, 1982; Ryugo & Sento, 1996; Ryugo *et al*., 1996, 1997, 1998), chinchillas (Lenn & Reese, 1966), guinea pigs (Gulley *et al*., 1978), and rats (Lenn & Reese, 1966; Rees *et al*., 1985). These large endings are characterized by clear, round synaptic vesicles and numerous, punctate asymmetric thickenings. The signature feature of endbulb synapses in mammals is the prominent dome-shaped PSDs.

This study also demonstrated that congenitally deaf *shaker-2* (*sh2/sh2*) mice exhibit clear and quantifiable abnormalities in endbulb morphology when compared to hearing littermates (+/*sh2* and +/+). There are smaller numbers of synaptic vesicles, a diminished mitochondrial volume fraction in the presynaptic endbulbs, and a corresponding hypertrophy of PSDs in target spherical bushy cells. There is also a conspicuous loss of intercellular cisternae that are formed between pre- and postsynaptic membranes in the normal hearing mice.

We speculate that one consequence of the deafness in *shaker-2* mice is an abnormality in the receptors of the synaptic complex. The nature of this abnormality, however, is not known. Clearly, the presence of a normal auditory sound stream appears important to stabilize or maintain receptor distribution along the endbulb-spherical bushy cell interface. In congenital deafness, cells of the cochlear nucleus are deprived

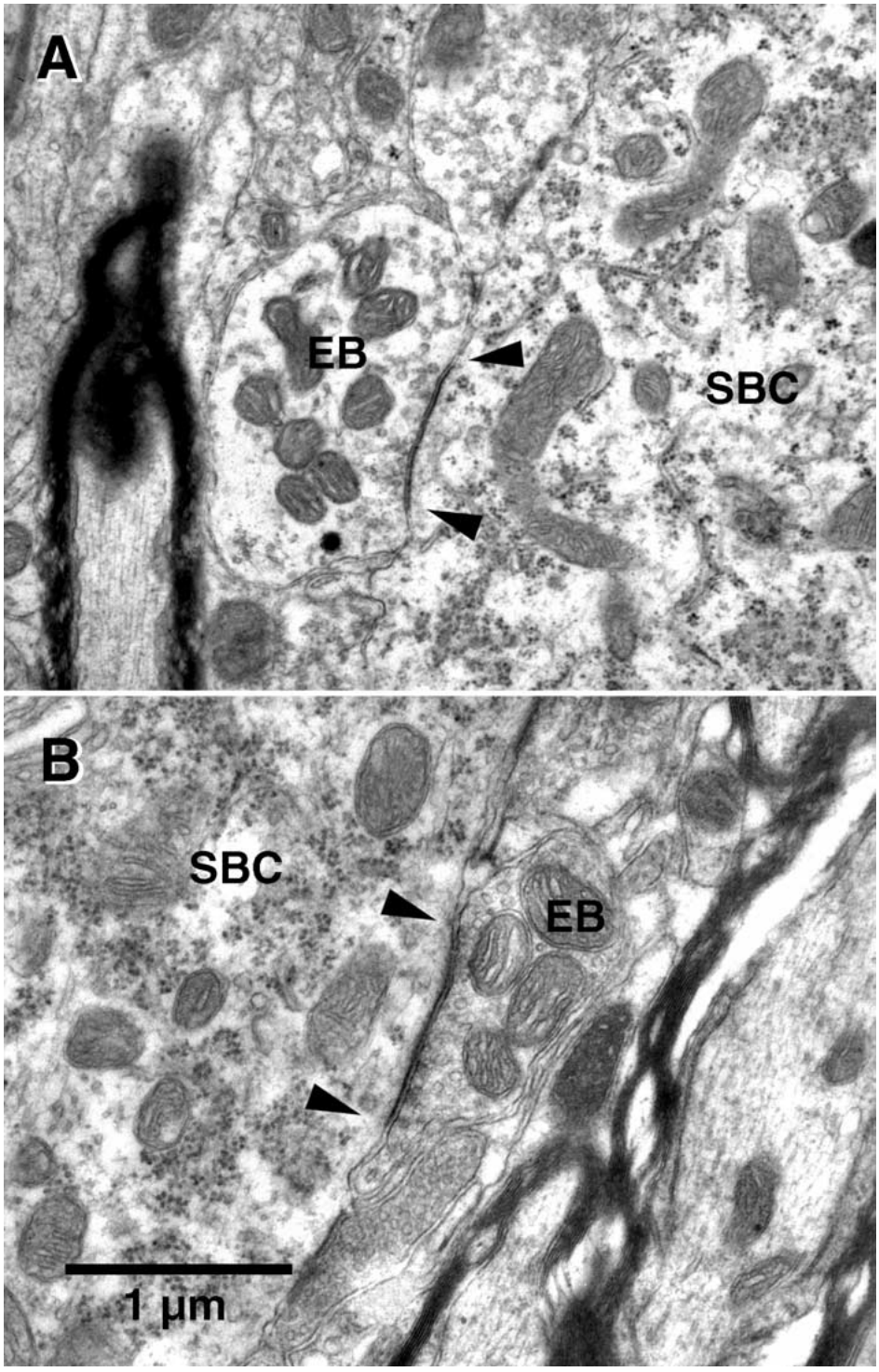

Fig. 6. Electron micrographs from 7 month old, homozygous deaf *sh2/sh2* mice. These micrographs were taken of endbulbs (EB) contacting spherical bushy cells (SBC) from different mice, and all showed characteristics typical of deaf animals. That is, there is a reduction of synaptic vesicles and a distinct hypertrophy of the PSD (arrowheads). The PSDs are flatter and longer than those observed in normal hearing littermates. There is also an absence of the intercellular cisternae that usually mark this synaptic interface in hearing animals. In these micrographs, ribosomes are darkly stained by lead citrate but have the same density as what we see in the hearing animals. Scale bar = 1.0 μm.

of action potentials, thereby eliminating voltage-gated membrane processes and reducing metabolic activity and blood flow. Using a rat model of transient cerebral ischemia, specific changes in protein composition as well as marked translocation of signaling molecules have been shown to accompany PSD thickening (Hu *et al.*, 1998). Could the PSD alterations observed in mutant mice and cats be secondary to "auditory ischemia?"

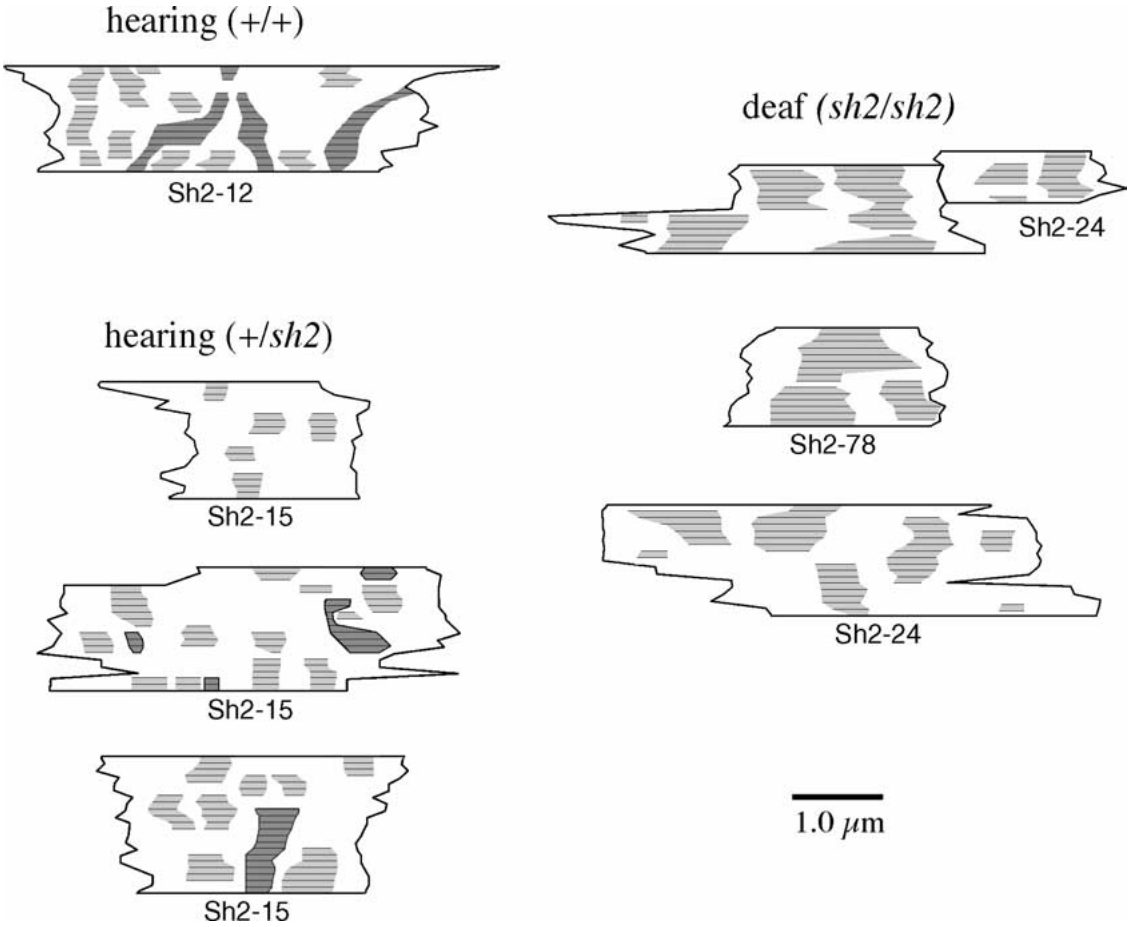

Fig. 7. Computer reconstructions of portions of endbulbs and their PSDs from normal hearing (+/+ and +/*sh2*) and deaf *(sh2/sh2)* mice. These reconstructions were rotated so that they are viewed *en face*. Each outline marks the SBC surface lying beneath a segment of the endbulb, and its mouse ID number provided below. The areas in light gray indicate the surface area of individual PSDs and the areas in darker gray mark the locations of intermembraneous channels or cisternae. The fine horizontal lines indicate individual sections. PSD area was increased in deaf mice compared with hearing littermates, suggesting a compensatory response to auditory deprivation. Intermembraneous channels were absent in deaf animals. Scale bar equals 1 μm.

Alternatively, studies on aminoglycoside-deafened rats revealed upregulation of glutamate receptor subunits GluR2/3 and NR1 in spiral ganglion cells (Hasegawa *et al*., 2000). These synaptic changes in the auditory periphery may correlate with central auditory pathway alterations as well.

At this point, it is relevant to address why we attribute these changes to surviving and not to degenerating auditory nerve fibers. It has been shown that auditory nerve fibers exhibit a characteristic and rapid degeneration pattern (Cohen, 1972; Gentschev & Sotelo, 1973; Cant & Morest, 1979; Tolbert & Morest, 1982). Following nerve section or cochlear ablation, primary terminals in the cochlear nucleus manifest several degenerative forms within 24–48 hours. The most common type is represented by a translucent and swollen appearance of the ending. There is a loss of synaptic vesicles, an appearance of vacuoles, and mitochondria swell. A second type exhibits marked swelling of the constituent synaptic vesicles accompanied by what appear as vesicle "shells" caused by a blurring of the vesicular membranes. The third type of degenerative process has been characterized as a "dark reaction." In this case, there is a kind of breakdown of neurofilaments and the accumulation of flocculent material in the ending that lead to dark and shrinking terminals. Within a week, the endings retract from the postsynaptic target, leaving uncovered PSDs. By approximately 10 days postlesion, the endings disappear. Since none of the endings analyzed in this report are associated with any of the above mentioned features, we conclude that we are analyzing remaining auditory nerve fibers that are intact and healthy.

The *sh2* mouse is a well-characterized model of autosomal recessive hearing loss, caused by a point mutation of *Myo15* on murine chromosome 11 (Probst *et al*., 1998). The abnormal stereocilia of the hair cell receptors are clearly visible by postnatal day 3 (Beyer *et al*., 2000), but the hair cells themselves remain more or less intact for the first several months (Deol, 1954). There are

Table 2. Endbulb data, comparing deaf, *sh2/sh2* mice with hearing, *+/sh2* and +/+ littermates.

Parameter	*Deaf mice (sh2/sh2)*	*Hearing mice (+/sh2, +/+)*	*P value*
Number of mice	3	5	N/A
Number of endbulbs	7	8	N/A
Number of profiles analyzed	64	91	N/A
Mitochondrial fraction (mitochondria silhouette area/profile area)	14 ± 5%	25 ± 7%	<0.001
Number of mitochondria per μm^2	1.65 ± 0.63	2.99 ± 0.91	<0.001
Synaptic vesicle density (vesicles/μm^2)	21 ± 9	77 ± 26	<0.001
Active zone fraction (PSD length/endbulb apposition length)	31 ± 0.11%	16 ± 0.03%	<0.001
Mean PSD area (μm^2)	0.23 ± 0.19 ($n = 48$ PSDs)	0.07 ± 0.04 ($n = 65$ PSDs)	<0.001

(a) PSD, postsynaptic density.
(b) "Profile" refers to a section through an endbulb. Multiple sections were collected from each endbulb.
(c) Apposition length refers to the surface contact between the endbulb and cell body (a linear measurement).
(d) Means ± standard deviations are provided.
(e) p values determined by ANOVA.

no other obvious phenotypic expressions of this mutation other than deafness and circling behavior, and these are evident by postnatal days 14–16 (Probst *et al*., 1998; Beyer *et al*., 2000). Accordingly, the central effects on auditory nerve synapses may be attributed to deafness (Ryugo *et al*., 1997, 1998; Redd *et al*., 2000). It should be noted that the *sh2/sh2* mice exhibited no ABR response at the earliest age tested (28 days after birth, unpublished observations). We infer that the absence of auditory stimulation during development

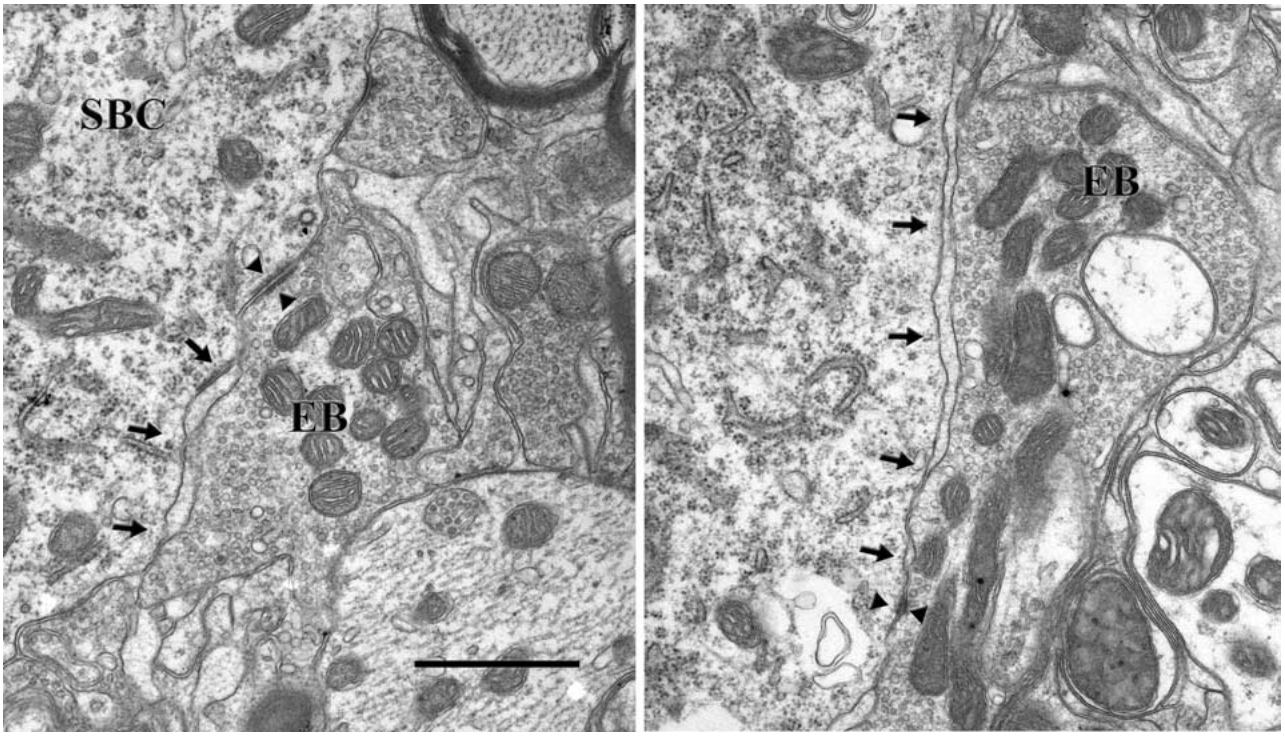

Fig. 8. High magnification electron micrographs of endbulb profiles from 7 month old, normal hearing mice *(+/sh2)*. The arrows delineate a stretch of separation of the pre- and postsynaptic membranes between the endbulb and spherical bushy cell. These separations form intercellular cisternae or channels that are common in hearing mice but rarely observed in deaf littermates. The arrowheads highlight *puncta adherentia*. *Puncta adherentia* are distinguished from postsynaptic densities by their symmetric projections into both the pre- and postsynaptic cytosol. Note the numerous round vesicles and abundant mitochondria. Scale bar equals 1.0 μm.

causes the structural alterations of synaptic elements between endbulbs of the auditory nerve and bushy cells of the cochlear nucleus.

The structural changes in the cochlea are virtually identical to what has been reported for humans (Scheibe, 1892) and the congenitally deaf white cat (Ryugo *et al*., 1997, 2003), where Reissner's membrane collapses onto the organ of Corti and obliterates the scala media. The similarities in central synapse pathology in cats and mice despite the different causes of deafness imply that these changes are caused by deafness itself and not some other nonspecific variable. On the other hand, it is entirely possible that the point mutation could be the same for the shaker mice and congenitally deaf white cats.

Deafness clearly exerts a powerful influence on brain development (Webster & Webster, 1981; Trune, 1982a,b; Webster, 1982, 1985; Rubel *et al*., 1990). The specific changes in auditory nerve synapses seem to represent a shared response to endbulb inactivity. There are several implications to this conclusion. First is that these abnormalities may not be restricted to the cochlear nucleus. The cochlear nucleus gives rise to the ascending auditory pathways so there could be widespread transneuronal alterations throughout higher auditory centers. Indeed, changes in cell body size, axon projections, and physiological responses have been reported in higher auditory structures in deaf white cats (West & Harrison, 1973; Schwartz & Higa, 1982; Nordeen *et al*., 1983; Moore & Kowalchuk, 1988; Kral *et al*., 2000). Accordingly, auditory nerve synapses altered by sensory deprivation have been implicated in the cascade of effects on the processing of acoustic information. Second, auditory stimulation during some developmental "critical" period appears essential for maintaining the structural and functional integrity of the central pathways (Parks, 1979; Webster & Webster, 1979; Webster, 1983; Rubel *et al*., 1984, 1990; Mostafapour *et al*., 2000). The notion of a critical period has been applied to explain phenomena that are affected most severely during a restricted time window of development (Ryugo *et al*., 2000; Rubel & Fritzsch, 2002). These critical periods emphasize that there are defined times when the physiological status of an organism is highly susceptible to an absence of certain environmental experiences. Third, these kinds of deafness-induced changes could provide insight into cellular mechanisms that underlie the variability in outcomes for humans using cochlear implants. These kinds of data could impact the prognosis of clinical intervention strategies as applied to congenitally deaf individuals. Congenital deafness most certainly interferes with the acquisition of spoken language in humans by breaking the auditory feedback loop. Analysis of cochlear implant data for prelingually deafened individuals suggests that young children represent the best candidates for auditory rehabilitation because delayed implantation predicts lower levels of speech recognition (Quittner & Steck, 1991; Waltzman *et al*., 1992; Gantz *et al*., 1994; Tyler & Summerfield, 1996; Tucci & Niparko, 2000).

The size of the endbulb and its numerous synaptic release sites are specialized features presumed to allow for high fidelity processing required in sound localization and speech comprehension. In human cochlear implantation, age of onset and duration of deafness are significant factors in predicting successful word recognition postoperatively (Rubinstein *et al*., 1999). Clarifying the time-course of synaptic development in endbulbs and documenting the impact of deafness on the central auditory system will be relevant in planning and justifying the timing of cochlear implantation in children and adults. Indeed, young patients or those postlingually deafened (after acquiring language skills) undergoing implantation enjoy superior speech comprehension compared to older patients who are prelingually deafened (Waltzman *et al*., 1992; Gantz *et al*., 1994; Waltzman *et al*., 1994). These clinical observations imply that early acoustic experience may minimize those sound-sensitive changes within endbulb synapses of the cochlear nucleus.

Acknowledgments

The authors gratefully thank Mr. Tan Pongstaporn for his expert technical assistance with the electron microscopy, Dr. Charles Limb for advice on mouse surgery, Alison Wright for helpful comments on the manuscript, and Michael Muniak for measurements of mitochondria. Portions of these data were presented in preliminary form at the 24th Annual Midwinter Research Meeting for the Association for Research in Otolaryngology, February 4–8, 2001. Grant sponsors: NIH/NIDCD DC00232 and DC00023, and the National Organization for Hearing Research Foundation.

References

ANDERSON, D. W., PROBST, F. J., BELYANTSEVA, I. A., FRIDELL, R. A., BEYER, L., MARTIN, D. M., WU, D., KACHAR, B., FRIEDMAN, T. B., RAPHAEL, Y. & CAMPER, S. A. (2000) The motor and tail regions of myosin XV are critical for normal structure and function of auditory and vestibular hair cells. *Hum. Mol. Genet*. **9**, 1729–1738.

BENES, F. M., PARKS, T. N. & RUBEL, E. W. (1977) Rapid dendritic atrophy following deafferentation: An EM morphometric analysis. *Brain Res*. **122**, 1–13.

BENSON, T. E., RYUGO, D. K. & HINDS, J. W. (1984) Effects of sensory deprivation on the developing mouse olfactory system: A light and electron microscopic, morphometric analysis. *J. Neurosci*. **4**, 638–653.

BERGSMA, D. & BROWN, K. (1971) White fur, blue eyes, and deafness in the domestic cat. *J. Hered*. **62**, 171–185.

BEYER, L. A., ODEH, H., PROBST, F. J., LAMBERT, E. H., DOLAN, D. F., CAMPER, S. A., KOHRMAN, D.

C. & RAPHAEL, Y. (2000) Hair cells in the inner ear of the pirouette and shaker 2 mutant mice. *J. Neurocytol*. **29**, 227–240.

BINNS, K. E., WITHINGTON, D. J. & KEATING, M. J. (1992) Post-crucial period effects of auditory experience and deprivation on the guinea-pig superior collicular map of auditory space. *Eur. J. Neurosci*. **4**, 1333–1342.

BOSHER, S. & HALLPIKE, C. (1965) Observations on the histological features, development and pathogenesis of the inner ear degeneration of the deaf white cat. *Proc. Roy. Soc. B* **162**, 147–170.

BURKARD, R. (1984) Sound pressure level measurement and spectral analysis of brief acoustic transients. *Electroenceph. clin. Neurophysiol*. **57**, 83–91.

CANT, N. B. & MOREST, D. K. (1979) The bushy cells in the anteroventral cochlear nucleus of the cat. A study with the electron microscope. *Neurosci.* **4**, 1925–1945.

COHEN, E. S. (1972) Synaptic organization of the caudal cochlear nucleus of the cat: A light and electron microscopical study. Doctoral Thesis, Cambridge, MA: Harvard University.

DEITCH, J. S. & RUBEL, E. W. (1984) Afferent influences on brain stem auditory nuclei of the chicken: Time course and specificity of dendritic atrophy following deafferentation. *J. Comp. Neurol*. **229**, 66–79.

DEITCH, J. S. & RUBEL, E. W. (1989a) Rapid changes in ultrastructure during deafferentation-induced dendritic atrophy. *J. Comp. Neurol*. **281**, 234–258.

DEITCH, J. S. & RUBEL, E. W. (1989b) Changes in neuronal cell bodies in N. laminaris during deafferentation-induced dendritic atrophy. *J. Comp. Neurol*. **281**, 259–268.

DEOL, M. S. (1954) The anomalies of the labyrinth of the mutants varitint-waddler, shaker-2 and jerker in the mouse. *J. Genet*. **52**, 562–588.

ELKABES, S., CHERRY, J. A., SCHOUPS, A. A. & BLACK, I. B. (1993) Regulation of protein kinase C activity by sensory deprivation in the olfactory and visual systems. *J. Neurochem*. **60**, 1835–1842.

FEKETE, D. M., ROUILLER, E. M., LIBERMAN, M. C. & RYUGO, D. K. (1984) The central projections of intracellularly labeled auditory nerve fibers in cats. *J. Comp. Neurol*. **229**, 432–450.

GANTZ, B., TYLER, R., WOODWORTH, G., TYE-MURRAY, N. & FRYAUF-BERTSCHY, H. (1994) Results of multichannel cochlear implants in congenital and acquired prelingual deafness in children: Five year follow up. *Am. J. Otol*. **15**, 1–8.

GENTSCHEV, T. & SOTELO, C. (1973) Degenerative patterns in the ventral cochlear nucleus of the rat after primary deafferentation. An ultrastructural study. *Brain Res*. **62**, 37–60.

GOLD, J. I. & KNUDSEN, E. I. (1999) Hearing impairment induces frequency-specific adjustments in auditory spatial tuning in the optic tectum of young owls. *J. Neurophysiol*. **82**, 2197–2209.

GOODMAN, C. S. & SHATZ, C. J. (1993) Developmental mechanisms that generate precise patterns of neuronal connectivity. *Cell* **72**, 77–98.

GULLEY, R. L., LANDIS, D. M. D. & REESE, T. S. (1978) Internal organizaton of memebranes at endbulbs of Held in the anteroventral cochlear nucleus. *J. Comp. Neurol*. **180**, 707–742.

HASEGAWA, T., DOI, K., FUSE, Y., FUJII, K., UNO, Y., NISHIMURA, H. & KUBO, T. (2000) Deafness induced up-regulation of GluR2/3 and NR1 in the spiral ganglion cells of the rat cochlea. *Neuroreport* **11**, 2515–2519.

HU, B. R., PARK, M., MARTONE, M. E., FISCHER, W. H., ELLISMAN, M. H. & ZIVIN, J. A. (1998) Assembly of proteins to postsynaptic densities after transient cerebral ischemia. *J. Neurosci*. **18**, 625–633.

IBATA, Y. & PAPPAS, G. D. (1976) The fine structure of synapses in relation to the large spherical neurons in the anterior ventral cochlear (sic) of the cat. *J. Neurocytol*. **5**, 395–406.

JULIANO, S. L., ESLIN, D. E. & TOMMERDAHL, M. (1994) Developmental regulation of plasticity in cat somatosensory cortex. *J. Neurophysiol*. **72**, 1706–1716.

KILLACKEY, H. P., BELFORD, G., RYUGO, R. & RYUGO, D. K. (1976) Anomalous organization of thalamocortical projections consequent to vibrissae removal in the newborn rat and mouse. *Brain Res*. **104**, 309–315.

KRAL, A., HARTMANN, R., TILLEIN, J., HEID, S. & KLINKE, R. (2000) Congenital auditory deprivation reduces synaptic activity within the auditory cortex in a layer-specific manner. *Cereb. Cortex* **10**, 714–726.

LARSEN, S. A. & KIRCHOFF, T. M. (1992) Anatomical evidence of plasticity in the cochlear nuclei of deaf white cats. *Exp. Neurol*. **115**, 151–157.

LEAKE, P. A., HRADEK, G. T., REBSCHER, S. J. & SNYDER, R. L. (1997) Chronic intracochlear electrical stimulation induces selective survival of spiral ganglion neurons in neonatally deafened cats. *Hear. Res*. **54**, 251–271.

LENN, N. J. & REESE, T. S. (1966) The fine structure of nerve endings in the nucleus of the trapezoid body and the ventral cochlear nucleus. *Am. J. Anat*. **118**, 375–390.

LEVAY, S., WIESEL, T. N. & HUBEL, D. H. (1980) The development of ocular dominance columns in normal and visually deprived monkeys. *J. Comp. Neurol*. **191**, 1–51.

LIANG, Y., WANG, A., BELYANTSEVA, I. A., ANDERSON, D. W., PROBST, F. J., BARBER, T. D., MILLER, W., TOUCHMAN, J. W., JIN, L., SULLIVAN, S. L., SELLERS, J. R., CAMPER, S. A., LLOYD, R. V., KACHAR, B., FRIEDMAN, T. B. & FRIDELL, R. A. (1999) Characterization of the human and mouse unconventional myosin XV genes responsible for hereditary deafness DFNB3 and shaker 2. *Genomics* **61**, 243–258.

LIMB, C. J. & RYUGO, D. K. (2000) Primary axosomatic endings in the anteroventral cochlear nucleus of mice: Development and deafness. *JARO* **1**, 103–119.

LIPPE, W. R., STEWARD, O. & RUBEL, E. W. (1980) The effect of unilateral basilar papilla removal upon nucleus laminaris and magnocellularis of the chick examined with [3H]2-deoxy-D-glucose autoradiography. *Brain Res*. **196**, 43–58.

LORENTE DE NÓ, R. (1981) The Primary Acoustic Nuclei. New York: Raven Press.

MAIR, I. W. (1973) Hereditary deafness in the white cat. *Acta. Otolaryngol*. **314**, 1–48.

MEISAMI, E. (1978) Influence of early anosmia on the developing olfactory bulb. *Prog. Brain Res*. **48**, 211–230.

MOORE, D. R., HUTCHINGS, M. E., KING, A. J. & KOWALCHUK, N. E. (1989) Auditory brain stem of the

ferret: Some effects of rearing with a unilateral ear plug on the cochlea, cochlear nucleus, and projections to the inferior colliculus. *J. Neurosci*. **9**, 1213–1222.

MOORE, D. R. & KOWALCHUK, N. E. (1988) Auditory brainstem of the ferret: Effects of unilateral cochlear lesions on cochlear nucleus volume and projections to the inferior colliculus. *J. Comp. Neurol*. **272**, 503–515.

MOSTAFAPOUR, S. P., COCHRAN, S. L., DEL PUERTO, N. M. & RUBEL, E. W. (2000) Patterns of cell death in mouse anteroventral cochlear nucleus neurons after unilateral cochlea removal. *J. Comp. Neurol*. **426**, 561–571.

NEVILLE, H. & BAVELIER, D. (2002) Human brain plasticity: Evidence from sensory deprivation and altered language experience. *Prog. Brain Res*. **138**, 177–188.

NORDEEN, K. W., KILLACKEY, H. P. & KITZES, L. M. (1983) Ascending projections to the inferior colliculus following unilateral cochlear ablation in the neonatal gerbil, *Meriones unguiculatus*. *J. Comp. Neurol*. **214**, 144–153.

PARKS, T. N. (1979) Afferent influences on the development of the brain stem auditory nuclei of the chicken: Otocyst ablation. *J. Comp. Neurol*. **183**, 665–677.

POWELL, T. P. S. & ERULKAR, S. D. (1962) Transneuronal cell degeneration in the auditory relay nuclei of the cat. *J. Anat*. **96**, 219–268.

PROBST, F. J., CHEN, K. S., ZHAO, Q., WANG, A., FRIEDMAN, T. B., LUPSKI, J. R. & CAMPER, S. A. (1999b) A physical map of the mouse shaker-2 region contains many of the genes commonly deleted in Smith-Magenis syndrome (del17p11.2p11.2). *Genomics* **55**, 348–352.

PROBST, F. J., FRIDELL, R. A., RAPHAEL, Y., SAUNDERS, T. L., WANG, A., LIANG, Y., MORELL, R. J., TOUCHMAN, J. W., LYONS, R. H., NOBEN-TRAUTH, K., FRIEDMAN, T. B. & CAMPER, S. A. (1998) Correction of deafness in *shaker-2* mice by an unconventional myosin in a BAC transgene. *Science* **280**, 1444–1447.

PUJOL, R., REBILLARD, M. & REBILLARD, G. (1977) Primary neural disorders in the deaf white cat cochlea. *Acta Otolaryngol*. **83**, 59–64.

QUITTNER, A. L. & STECK, J. T. (1991) Predictors of cochlear implant use in children. *Am. J. Otol*. **12** (Suppl), 89–94.

REBILLARD, M., PUJOL, R. & REBILLARD, G. (1981b) Variability of the hereditary deafness in the white cat. II. *Histology. Hear. Res*. **5**, 189–200.

REBILLARD, M., REBILLARD, G. & PUJOL, R. (1981a) Variability of the hereditary deafness in the white cat. I. *Physiology. Hearing Res*. **5**, 179–181.

REDD, E. E., PONGSTAPORN, T. & RYUGO, D. K. (2000) The effects of congenital deafness on auditory nerve synapses and globular bushy cells in cats. *Hear. Res*. **147**, 160–174.

REES, S., GULDNER, F. H. & ATIKIN, L. (1985) Activity dependent plasticity of postsynaptic density structure in the ventral cochlear nucleus of the rat. *Brain Res*. **325**, 370–374.

RUBEL, E. W. (1984) Ontogeny of auditory system function. *Ann. Rev. Physiol*. **46**, 213–229.

RUBEL, E. W. & FRITZSCH, B. (2002) Auditory system development: Primary auditory neurons and their targets. *Ann. Rev. Neurosci*. **25**, 51–101.

RUBEL, E. W., HYSON, R. L. & DURHAM, D. (1990) Afferent regulation of neurons in the brain stem auditory system. *J. Neurobiol*. **21**, 169–196.

RUBINSTEIN, J. T., PARKINSON, W. S., TYLER, R. S. & GANTZ, B. J. (1999) Residual speech recognition and cochlear implant performance: Effects of implantation criteria. *Am. J. Otol*. **20**, 445–452.

RYUGO, D. K., CAHILL, H. B., ROSE, L. S., ROSENBAUM, B. T., SCHROEDER, M. E., & WRIGHT, A. L. (2003) Separate forms of pathology in the cochlea of congenitally deaf white cats. *Hear. Res*.

RYUGO, D. K. & FEKETE, D. M. (1982) Morphology of primary axosomatic endings in the anteroventral cochlear nucleus of the cat: A study of the endbulbs of Held. *J. Comp. Neurol*. **210**, 239–257.

RYUGO, D. K., LIMB, C. J. & REDD, E. E. (2000) Synaptic plasticity: The impact of the environment on the brain as it relates to cochlear implants. In *Cochlear Implants: Principles and Practices* (edited by Niparko, J. K., Kirk, K. I., Mellon, N. K., Robbins, A. M., Tucci, D. L. & Wilson, B. S.) pp. 33–56. Philadelphia: Lippincott Williams & Williams.

RYUGO, D. K. & PARKS, T. N. (2003) Innervation of the cochlear nucleus in birds and mammals. *Brain Res. Bull*. **60**, 435–456.

RYUGO, D. K., PONGSTAPORN, T., HUCHTON, D. M. & NIPARKO, J. K. (1997) Ultrastructural analysis of primary endings in deaf white cats: Morphologic alterations in endbulbs of Held. *J. Comp. Neurol*. **385**, 230–244.

RYUGO, D. K., ROSENBAUM, B. T., KIM, P. J., NIPARKO, J. K. & SAADA, A. A. (1998) Single unit recordings in the auditory nerve of congenitally deaf white cats: Morphological correlates in the cochlea and cochlear nucleus. *J. Comp. Neurol*. **397**, 532–548.

RYUGO, D. K. & SENTO, S. (1996) Auditory nerve terminals and cochlear nucleus neurons: Endbulbs of Held and spherical bushy cells. In *Advances in Speech, Hearing and Language Processing* (edited by Ainsworth, W. A.), pp. 19–40. London: Jai Press Ltd.

RYUGO, D. K., WU, M. M. & PONGSTAPORN, T. (1996) Activity-related features of synapse morphology: A study of endbulbs of Held. *J. Comp. Neurol*. **365**, 141–158.

SAADA, A. A., NIPARKO, J. K. & RYUGO, D. K. (1996) Morphological changes in the cochlear nucleus of congenitally deaf white cats. *Brain Res*. **736**, 315–328.

SCHEIBE, A. (1892) A case of deaf-mutism, with auditory atrophy and anomalies of development in the membranous labyrinth of both ears. *Arch. Otolaryngol*. **21**, 12–22.

SCHWARTZ, I. R. & HIGA, J. F. (1982) Correlated studies of the ear and brainstem in the deaf white cat: Changes in the spiral ganglion and the medial superior olivary nucleus. *Acta Otolaryngol*. **93**, 9–18.

SHENG, M. (2001) Molecular organization of the postsynaptic specialization. *Proc. Natl. Acad. Sci*. **98**, 7058–7061.

SUGA, F. & HATTLER, K. W. (1970) Physiological and histopathological correlates of hereditary deafness in animals. *Laryngoscope* **80**, 81–104.

TIBUSSEK, D., MEISTER, H., WALGER, M., FOERST, A. & VON WEDEL, H. (2002) Hearing loss in early infancy

affects maturation of the auditory pathway. *Dev. Med. Child Neurol.* **44**, 123–129.

TOLBERT, L. P. & MOREST, D. K. (1982c) The neuronal architecture of the anteroventral cochlear nucleus of the cat in the region of the cochlear nerve root: Electron microscopy. *Neurosci*. **7**, 3053–3067.

TRUNE, D. R. (1982a) Influence of neonatal cochlear removal on the development of mouse cochlear nucleus: I. Number, size, and density of its neurons. *J. Comp. Neurol*. **209**, 409–424.

TRUNE, D. R. (1982b) Influence of neonatal cochlear removal on the development of mouse cochlear nucleus: II. Dendritic morphometry of its neurons. *J. Comp. Neurol*. **209**, 425–434.

TUCCI, D. L. & NIPARKO, J. K. (2000) Medical and surgical aspects of cochlear implantation. In *Cochlear Implants: Principles and Practices* (edited by Niparko, J. K., Kirk, K. I., Mellon, N. K., Robbins, A. M., Tucci, D. L. & Wilson, B. S.) pp. 189–221. New York: Lippincott Williams & Wilkins.

TYLER, R. S. & SUMMERFIELD, A. Q. (1996) Cochlear implantation: Relationships with research on auditory deprivation and acclimatization. *Ear Hear*. **17** (Suppl), 38s–50s.

VAN DER LOOS, H. & WOOLSEY, T. A. (1973) Somatosensory cortex: Structural alterations following early injury to sense organs. *Science* **179**, 395–398.

WALTZMAN, S., FISHER, S., NIPARKO, J. K. & COHEN, N. (1994) Predictors of postoperative performance with cochlear implants. *Ann. Otol. Rhinol. Laryngol*. **104**, 15–18.

WALTZMAN, S. B., COHEN, N. L. & SHAPIRO, W. H. (1992) Use of a multichannel cochlear implant in the congenitally and prelingually deaf population. *Laryngoscope* **102**, 395–399.

WEBSTER, D. B. (1983a) A critical period during postnatal auditory development of mice. *Int. J. Pediatr. Otorhinolaryngol*. **6**, 107–118.

WEBSTER, D. B. (1985) The spiral ganglion and cochlear nuclei of deafness mice. **18**, 19–27.

WEBSTER, D. B., SOBIN, A. & ANNIKO, M. (1986) Incomplete maturation of Brainstem auditory nuclei in genetically induced early postnatal cochlear degeneration. *Acta Otolaryngol*. **101**, 429–438.

WEBSTER, D. B. & TRUNE, D. R. (1982) Cochlear nuclear complex of mice. *Am. J. Anat*. **163**, 103–130.

WEBSTER, D. B. & WEBSTER, M. (1979) Effects of neonatal conductive hearing loss on brainstem auditory nuclei. *Ann. Otol. Rhinol. Laryngol*. **88**, 684–688.

WEBSTER, M. & WEBSTER, D. B. (1981) Spiral ganglion neuron loss following organ of Corti loss: A quantitative study. *Brain Res*. **212**, 17–30.

WEST, C. D. & HARRISON, J. M. (1973) Transneuronal cell atrophy in the deaf white cat. *J. Comp. Neurol.* **151**, 377–398.

WIESEL, T. N. & HUBEL, D. H. (1963) Effects of visual deprivation on morphology and physiology of cells in the cat's lateral geniculate body. *J. Neurophysiol*. **26**, 973–993.

WILLARD, F. H. & RYUGO, D. K. (1983) Anatomy of the central auditory system. In *The Auditory Psychobiology of the Mouse* (edited by Willott, J. F.) pp. 201–304. Springfield, IL: Charles C. Thomas.